Synthesis and Characterization of Thermotropic Liquid Crystalline Poly(ester-imide-ketone)

Zhenguo Chi, Jiarui Xu

Key Laboratory for Polymeric Composite and Functional Materials of Ministry of Education, Materials Science Institute, Sun Yat-sen (Zhongshan) University, Guangzhou, 510275, China

Received 27 September 2002; accepted 2 February 2003

ABSTRACT: A series of poly(ester imide ketone)s derived from *N,N′*-hexane-1,6-diylbis(trimellitimide), 4,4′-dihydroxybenzophenone, and *p*-hydroxybenzoic acid (PHB) were synthesized by the direct polycondensation method in benzene sulfonyl chloride, dimethylformamide, and pyridine with varied PHB contents. The liquid crystalline behavior and thermal properties of the poly(ester imide ketone)s were characterized by polarized-light microscopy, wide-angle X-ray diffraction, thermogravimetric analysis, differential scanning calorimetry, and temperature-modulated differential scanning calorimetry (MDSC). The results showed that the synthesized polymers possessed a nematic thermotropic liquid crystalline characteristic and high thermal stability. The liquid crystalline polymers, with a PHB content ranging from 0 to 50 mol %, exhibited multiple phase transitions as evidenced by the MDSC results. A transitional smectic phase from solid state to nematic thermotropic liquid crystalline state was observed, and a transition model is proposed. Under certain conditions, the polymer with 33 mol % PHB content showed two significantly different liquid crystalline textures. This type of liquid crystalline polymer exhibited excellent fiber forming. © 2003 Wiley Periodicals, Inc. J Appl Polym Sci 90: 1045–1052, 2003

Key words: poly(ester imide ketone); liquid crystalline polymer (LCP); polycondensation; phase behavior

INTRODUCTION

Thermotropic liquid crystalline poly(ester imide)s (TLCPEIs) have attracted a great deal of attention since 1987, when the liquid crystalline character of poly(ester imide) was first reported by Kricheldorf.[1] Some approaches for synthesizing poly(ester imide)s have been explored, such as (1) melt transesterification via the carboxylic acid (or hydroxyl) group of a monomer containing a built-in imide ring with a hydroxyl (or carboxylic acid) group of the other monomers; and (2) solution polycondensation via a dianhydride containing a preformed ester group with a diamine. Both these procedures involved the reaction of an anhydride group of trimellitic anhydride with the amino group of a diamine or amino alcohol or amino acid in the first or final stage. Yet, as far as is known, nearly all reported TLCPEIs with higher molecular weights have been synthesized by the melt transesterification approach at high temperature under reduced pressure. This might be practical from an industrial standpoint but is too complicated for fundamental investigations of such aspects as the reaction mechanism and sequence structure. For this purpose, a polycondensation method developed by Higashi et al.[2] for aromatic polyesters in solution should be useful, as not only can high-molecular-weight polyarylesters be synthesized, but monomer sequences controlled in the copolycondensation process as well.

Until now, no articles have been found in the literature that have reported using Higashi's method to synthesize poly(ester imide). Based on the principle of this method, a series of high-molecular-weight thermotropic liquid crystalline polyesters and TLCPEIs were synthesized in our laboratory. In this article we describe the detailed results of the synthesis and characterization of poly(ester imide ketone)s derived from *N,N′*-hexane-1,6-diylbis(trimellitimide), 4,4′-dihydroxybenzophenone, and *p*-hydroxybenzoic acid.

EXPERIMENTAL

Materials

4,4′-Dihydroxybenzophenone was synthesized from phenol and *p*-hydroxybenzoic acid according to the method of Stanley.[3] *N,N′*-Hexane-1,6-diylbis(trimellitimide) was synthesized from trimellitic anhydride and 1,6-hexane diamine according to the method detailed by Kricheldorf and Pakull.[4] All other materials

Correspondence to: J. Xu (cesxjr@zsu.edu.cn).

Contract grant sponsor: National Natural Science Foundation of China; contract grant numbers: 50133020 and 59625307.

Contract grant sponsor: Team Project of the Natural Science Foundation of Guangdong Province, China; contract grant number: 20003038.

Contract grant sponsor (to Jiarui Xu): Educational Bureau of Guangdong Province; contract grant number: Q02014.

Journal of Applied Polymer Science, Vol. 90, 1045–1052 (2003)

were obtained as chemical-grade reagents from a commercial source (Guangzhou Medicine Company, Guangzhou, China) and were used without further purification.

Polycondensation

A typical procedure for synthesis of poly(ester imide ketone) was used, as follows: 3.32 mL of benzene sulfonyl chloride (BsCl), 1.55 mL of dimethylformamide (DMF), and 10 mL of pyridine (Py) were taken by pipette into a 250-mL round-bottom flask with an electromagnetic stirrer. The mixture was aged at room temperature for 30 min. Then 5 mmol of *N,N′*-hexane-1,6-diylbis(trimellitimide) was weighed into the flask under stirring. After the resulting mixture became solidified, the flask was placed into an oil bath preheated to 80°C and was maintained there for 10 min. Then 10 mL of the Py solution, composed of 5 mmol of 4,4′-dihydroxybenzophenone and 10 mmol of *p*-hydroxybenzoic acid, was added to the above mixture drop by drop over about 10 min. The temperature was then rapidly raised to 120°C and maintained there for 2 h. After dilution with 20 mL of DMF, the precipitate was filtered and washed with alcohol. The filtered polymers were dried in a far-infrared oven. The mole content of PHB in the poly(ester imide ketone) obtained was 50%. The other poly(ester imide ketone)s, which had varied PHB contents, were synthesized using a similar procedure.

Characterization

The intrinsic viscosity, [η], of the polymers was determined at 30°C in phenol/*sym*-tetrachloroethane (PTCE; 60:40 by weight) at a concentration of 0.5 g/dL using an Ubbelohde viscometer.

The liquid crystalline texture of the resultant polymers was observed under a Leitz Orthoplan optical microscope equipped with cross-polarizers and a hot stage.

The wide-angle X-ray diffraction curves were measured with a Rigaku XD-3A diffractometer using Ni-filtered Cu Kα radiation and λ = 1.54 Å.

Thermogravimetric analysis (TGA) was performed in air using a Shimadzu TGA-50H at a heating rate of 20°C/min.

Differential scanning calorimetry (DSC) and temperature-modulated differential scanning calorimetry (MDSC) measurements were conducted with a TA

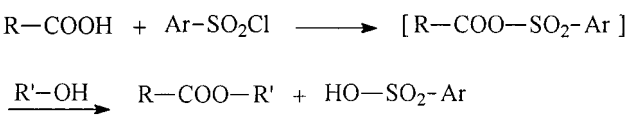

Scheme 1

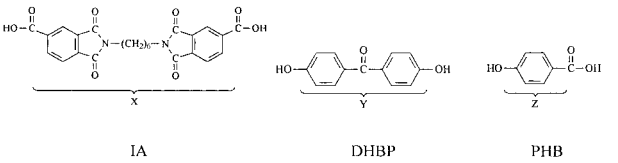

Scheme 2

Instruments MDSC 2910 under a nitrogen purge. For DSC measurements the scanning rate used was 10°C/min, whereas the MDSC experiments were performed at a scanning rate of 3°C/min, a temperature–modulation amplitude of ±0.5°C, and a modulation period of 30 s.

RESULTS AND DISCUSSION

Chemical structure and NMR characteristics

The main feature of Higashi's direct polycondensation method is that the dicarboxylic acid monomer is activated by BsCl to form a hybrid acid anhydride, and then the acid anhydride reacts with a bisphenol monomer to form the polyester. The model reaction is shown in Scheme 1. The structures of three monomers used in our report are given in Scheme 2.

As PHB monomer contains both hydroxyl and carboxyl groups, it can react not only with IA and DHBP but also can undergo self-polycondensation. Therefore, in this context, PHB and DHBP were mixed in Py and dropped into the activated dicarboxylic acid IA. The possible molecular structure of the resulting copolymer is schematically shown in Scheme 3.

The ^{1}H-NMR spectrum of the sample containing 33% PHB, determined in trifluoroacetic acid (CF_3COOD), is shown in Figure 1. The integrated ratios of the different protons and their chemical shifts are fully in conformity with the structure of the copolymer.

Intrinsic viscosity of the polymers

Theintrinsic viscosity, [η], of the polymers was determined at 30°C in phenol/*sym*-tetrachloroethane (PTCE, 60:40 by weight) at a concentration of 0.5 g/dL using an Ubbelohde viscometer. The [η] values are listed in the Table I. The sample with 67 mol % PHB could not dissolve in the above solvent.

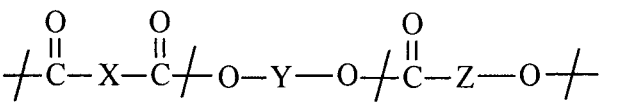

Scheme 3

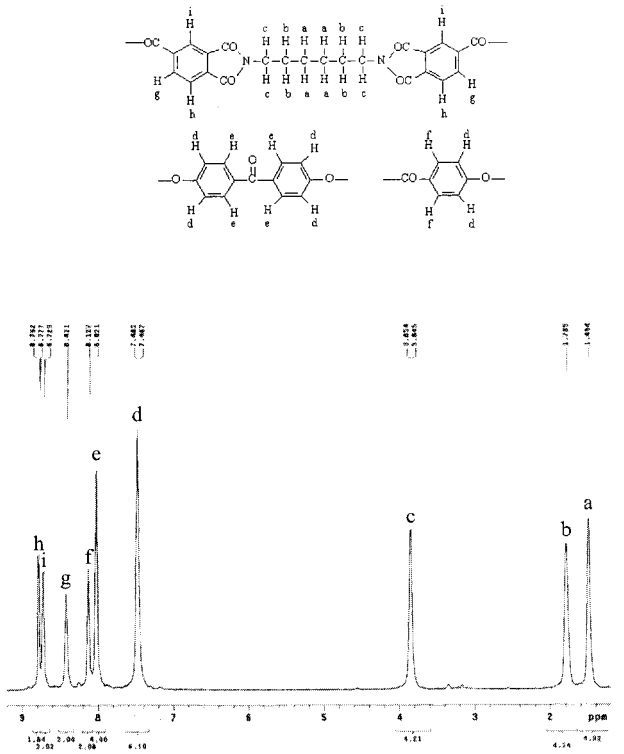

Figure 1 ^{1}H-NMR of the copolymer with 33% PHB (in CF_3COOD).

Observation by polarized-light microscopy

Under a polarizing-light microscope (PLM), polymers containing more than 20 mol % of PHB showed a very high degree of birefringence with threaded nematic texture in the molten state.

Upon stepwise increasing of the temperature, the transition processes from the solid to the nematic and then to the isotropic state could be clearly observed (Fig. 2). The transition temperature from the solid state to the nematic state for the polymer with 33% PHB was about 265°C, which corresponds to the T_m2 of the DSC results (shown later). And a phase transition from the nematic state to the complete isotropic state occurred at about 330°C.

When the temperature was raised to the nematic-to-isotropic transition temperature (T_i), it was observed that the birefringence of the polymers synthesized by this method disappeared completely (before the decomposition temperature, as T_d = 422°C at 5% weight loss), whereas for the polymers obtained by the melt transesterification approach, the disappearance of birefringence was not observed until the samples decomposed.[5]

TABLE I
Relationship of PHB Content and Intrinsic Viscosity

PHB (mol %)	0	11	20	33	50	67
[η] (dL/g)	0.51	0.62	0.58	0.90	0.70	—

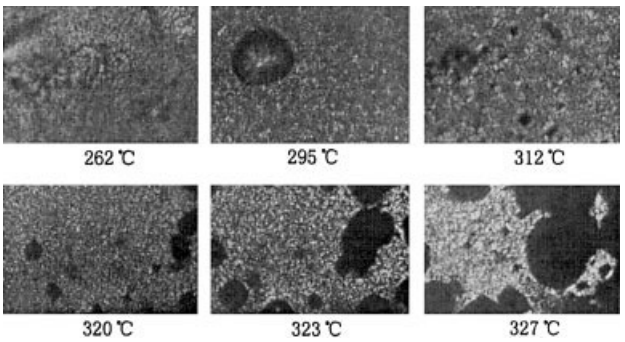

Figure 2 Polarizing microscope photographs of melting process of polymer with 33% mol PHB (X500).

Figure 3(a) is a polarizing microscope photograph of the polymer with 33% mol PHB after shearing from the melt. The typical sheared nematic Schlieren texture was clearly observed.

Very interestingly, under certain conditions it was possible to obtain a texture like a spherulite [Fig. 3(b)], which is completely different from that shown in Figure 3(a). After a heating (from room temperature to 330°C) and cooling (from 330°C to room temperature, ca. 2 min) cycle process, it was found that this texture disappeared and changed into thread texture completely under PLM observation at room temperature. This probably indicates that the formation of the texture was greatly temperature dependent.

Although all samples experienced a shearing process in the molten state, the sheared nematic Schlieren texture could not be observed once the texture like spherulite formed [see Fig. 3(b)]. In other words, the macromolecules could not be oriented in the conditions in which the texture was formed. This is very important from the viewpoint of polymer processing. Unfortunately, until now, the means of precisely controlling the formation conditions of the texture were not clear, and further studies are still under way.

The relationship between PHB content and liquid crystalline properties is summarized in Table II. As expected, the degree of birefringence was strengthened with an increase in PHB content. The results also

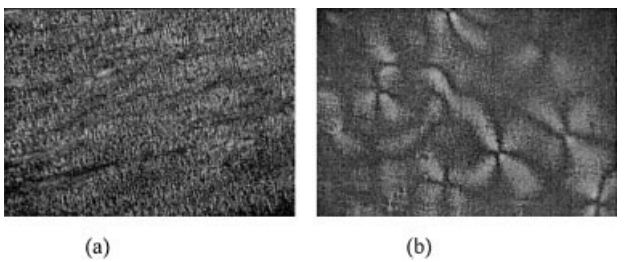

Figure 3 Polarizing microscope photographs of polymer with 33% mol PHB at sheared state (X500).

TABLE II
Relationship of PHB Content and Liquid–Crystalline Properties

PHB (mol %)	0	11	20	33	50	67
Birefringence	Weak	Weak	Middle	Very strong	Very strong	Very strong
Morphology	Thread	Thread	Thread	Thread	Thread	Thread
Forming shared Schlieren texture	Difficult	Difficult	Easy	Easy	Very easy	Very easy
Forming fiber from melt state	Difficult	Difficult	Difficult	Easy	Easy	Difficult

show that the polymers whose PHB content were 33% and 50% had good fiber-forming ability. Therefore, the ability to form liquid crystalline fibers could be tailored by controlling PHB content during polymer synthesis.

Wide-angle X-ray diffraction

Figures 4 and 5 show the wide-angle X-ray diffraction (WAXD) patterns of, respectively, as-synthesized powder samples and melt-pressed samples (naturally cooled from room temperature). From Figure 4 it can be seen that all the as-synthesized samples show an evident degree of crystallinity, as indicated by several strong diffraction peaks in the range of $2\theta = 20°–30°$. With the decrease of PHB content, the diffraction intensity increases. And for the sample with PHB content less than 33%, several weak diffraction peaks can also be observed at lower angles (ca. $2\theta = 10°$), probably indicating that these polymers form a layer structure in the solid state, as suggested by Kricheldorf.[1]

After melt pressing the WAXD patterns exhibited characteristic nematic diffraction, with a diffused peak at about $2\theta = 20°$ and several shoulder peaks around (Fig. 5). The diffraction peaks at lower angles disappeared, indicating that the crystal structure changed after the melt-pressing treatment. The DSC results, explained below, also confirmed such a change.

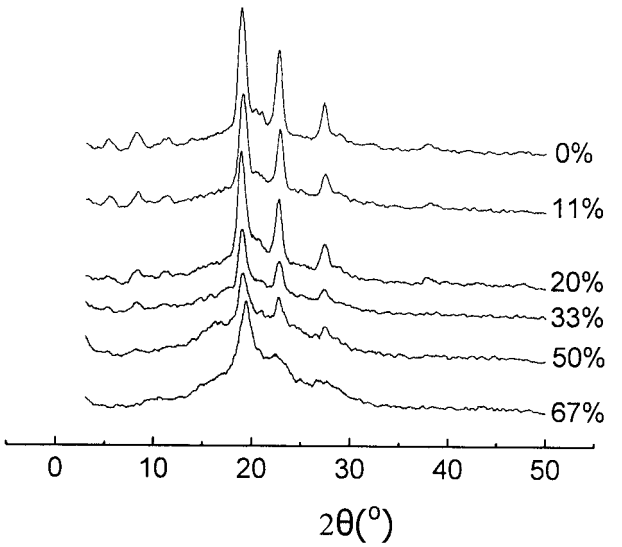

Figure 4 WAXD patterns of as-synthesized polymers.

TGA measurement

The thermal stability of the obtained poly(ester imide ketone)s was evaluated by TGA, which was performed in air at a heating rate of 20°C/min. Typical TGA curves of the polymers of different PHB contents are shown in Figure 6. The decomposition temperatures for 5% weight loss ranged from 413°C to 432°C, indicating the onset of significant thermal degradation of the polymers. The TGA data are listed in Table III. There was no significant difference in thermal stability between the polymers with different PHB contents. All the polymers showed high thermal stability.

DSC and MDSC measurements

All the as-synthesized poly(ester imide ketone) powders were subjected to DSC measurement at a heating and cooling rate of 10°C/min in the temperature range of 50°C–300°C, as shown in Figures 7–9.

In the DSC traces, the nematic-to-isotropic transition temperature (T_i) was not detectable.

The glass-transition temperatures (T_g) could not be detected in the first heating scan in all cases, but it could be observed in the cooling and second heating runs because of the increase in the amorphous fraction after the melting and cooling processes. These results correspond to the WAXD results, mentioned above. The T_g values taken from the second heating scans are listed in Table IV. Clearly, the T_g values decreased

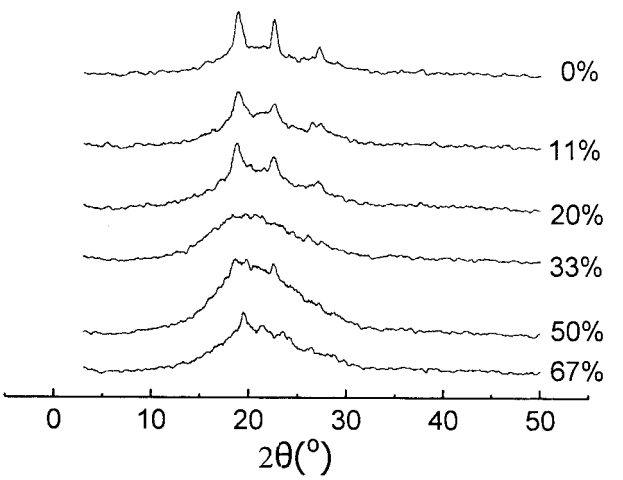

Figure 5 WAXD patterns of melt-pressed samples of the polymers.

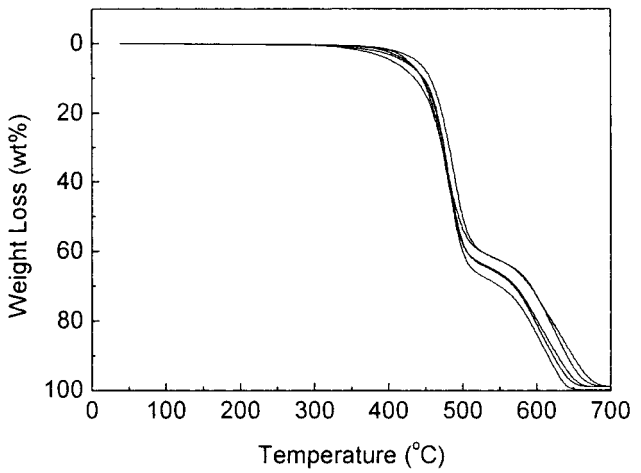

Figure 6 TGA curves of polymers with different contents of PHB.

linearly with increasing mole percentage of PHB, probably because of the decrease in the degree of homopolymerization with an increase in PHB content in the range of 0%–67%.

In the first heating run the samples with a PHB content of 0%–33% showed two endothermic peaks between 250°C–300°C. In the cooling run the samples with a PHB content of 0%–20% showed only one exothermic peak, whereas for the second heating run, the samples with a PHB content of 0%–50% had two endothermic peaks. It is worth noting that the first endothermic peak area (T_m1) lessened and the second endothermic peak area (T_m2) enlarged. After the first heating and cooling runs, the sample with 50% PHB also showed two endothermic peaks in the second heating run. Comparing the first heating curve with the second heating one, it is evident that not only did the shape of the T_m1 change, but its position also shifted, whereas the position of T_m2 did not shift visibly.

The recently developed temperature-modulated differential scanning calorimetry (MDSC) has made a substantial impact on the ability to measure various thermal responses and on the understanding of their underlying kinetics and thermodynamics.[6] It is an important merit of the MDSC method that it allows simultaneous measurement and subsequent deconvolution of reversing and nonreversing thermal effects. For example, one can measure such nonreversing effects as the enthalpy relaxation during the glass transition, heats of chemical reaction, and heats of fusion and separate them quantitatively from the reversing heat capacity. The reversible thermodynamic heat capacity always provides the baseline for the quantitative evaluation of these nonreversing effects.

To get further verification of the results obtained from PLM, WAXD, and DSC, MDSC measurements were conducted.

The following multiple heating and cooling sequences were designed and run for four samples with 33% PHB ([η] = 0.90 dL/g; Figs. 10–12).

(a) as-synthesized sample $\xrightarrow{\text{Heated quickly from 50°C}}$ 200°C and isothermal 5min $\xrightarrow{3°C/min}$ 300°C

(b) as-synthesized sample $\xrightarrow{\text{Heated quickly from 50°C}}$ 300°C and isothermal 5min $\xrightarrow{-3°C/min}$ 50°C and isothermal 1 min $\xrightarrow{3°C/min}$ 300°C →

(c) isothermal 5min $\xrightarrow{\text{cooled quickly from 300°C}}$ 50°Cand isothermal 1 min $\xrightarrow{3°C/min}$ 300°C →

(d) isothermal 5min $\xrightarrow{-3°C/min}$ 50°C and isothermal 1 min $\xrightarrow{3°C/min}$ 300°C

Figure 10 shows the total heat flow (THF), which is equivalent to the conventional DSC measurement. Comparing the results from MDSC with DSC, although the same as-synthesized samples (with 33% PHB content) were both obtained from the first heating process, their shapes and positions are obviously different: (1) in Figure 7 (the 33% PHB curve) it is clear that the peak area of T_m1 is larger than that of T_m2; but in Figure 10, curve a, there is no observable difference between T_m1 and T_m2; (2) Tables IV and V show that

TABLE III
Dependence of TGA Data on PHB Content

PHB (mol %)	0	11	20	33	50	67
TGA temperature (°C) (weight loss 5%)	430.5	432.0	425.8	422.5	429.2	413.5
TGA temperature (°C) (at max decomposed rate)	480.4	481.9	471.7	469.3	476.8	479.3

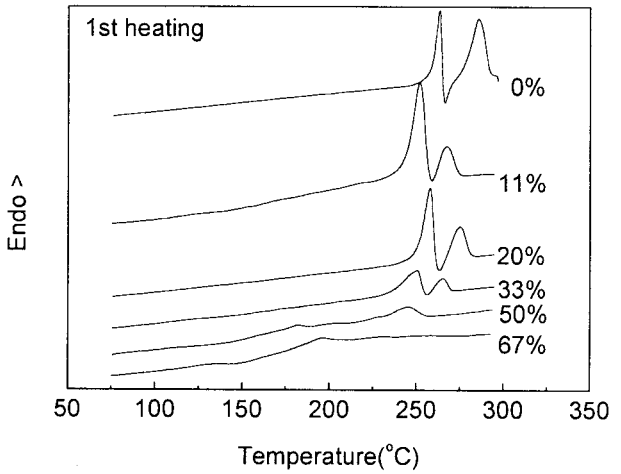

Figure 7 DSC curves of polymers on first heating.

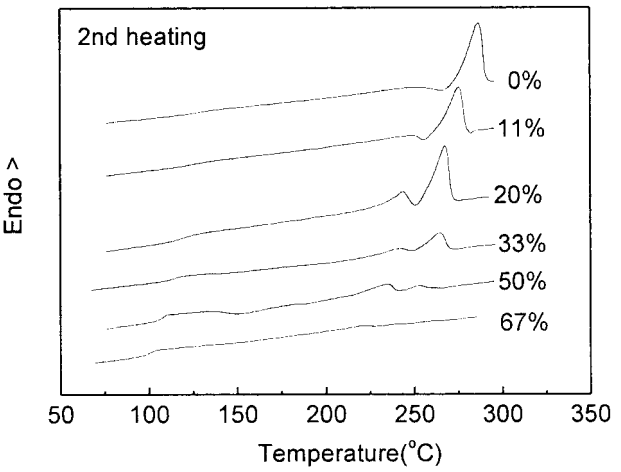

Figure 9 DSC curves of polymers on second heating.

the values of T_m1 and T_m2 from MDSC are lower than those from DSC: the difference in the values is about 5°C for T_m1 and less 1°C for T_m2.

The above comparison shows that the thermal history had a significant effect on the transition temperatures and their enthalpies. Moreover, the T_m1 transition was more sensitive to thermal treatment than was that of the T_m2. This suggests that the stability of the aggregation state related to T_m1 was lower than that of T_m2. That is to say, it probably formed a higher dimensional aggregation structure under T_m1.

We therefore speculated that the T_m1 peak corresponds to a transition from the three-dimensional crystalline state to the two-dimensional smectic state and that the T_m2 peak is related to a transition from the two-dimensional smectic state to the one-dimensional nematic state. It should be noted that the T_m2 peak is not the transition temperature (T_i) from the nematic state to the isotropic state, as the T_i was about 330°C, according to the PLM results mentioned above.

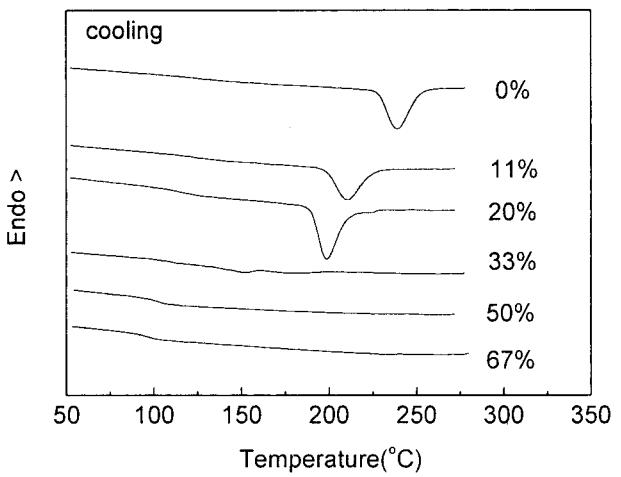

Figure 8 DSC curves of polymers on cooling.

To test the above speculation, Procedures b, c, and d were carried out. In fact, Procedure b is equivalent to the second heating run in the DSC scan, and both curves were similar (the DSC curve of 33% PHB in Fig. 8 and curve b in Fig. 10). The same result was observed: the T_m1 peak area became less pronounced, but the T_m2 peak remained nearly unchanged, suggesting that after the heating and cooling runs, the number of crystals formed under T_m1 was less than that formed during the first heating run, but the number of smectic microcrystallites formed under T_m2 remained almost unchanged. This also implies that the formation of crystalline aggregation under T_m1 was more difficult than the formation of smectic aggregation under T_m2, apparently because the sample used in Procedure a was an as-synthesized sample precipitated directly from the solution and the sample used in Procedure b had experienced a melting process. It is well known that polymers may grow three-dimensional crystals more easily in solution than in the melt because of the lower viscosity of the system. The unchanged peak area of T_m2 transition therefore suggests

TABLE IV
Transition Temperatures of Polymers with Different Heating Procedures

Procedure	PHB content (mol %)	T_g (°C)	T_m1 (°C)	T_m2 (°C)
1st heating	0	—	263.3	285.6
	11	—	257.6	275.1
	22	—	252.0	268.1
	33	—	250.6	265.8
	50	—	245.6	—
	67	—	—	—
2nd heating	0	128.7	253.5	286.6
	11	122.0	250.1	275.4
	20	117.4	243.6	267.7
	33	113.6	241.9	264.7
	50	108.3	235.5	252.9
	67	100.9	—	—

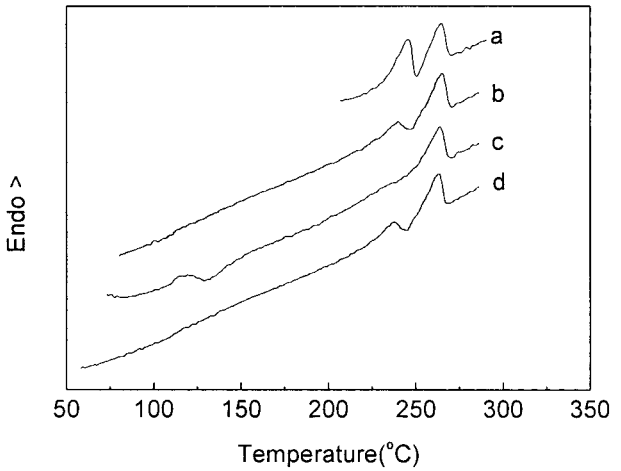

Figure 10 MDSC curves of 33% PHB polymer using different procedures (total heat flow).

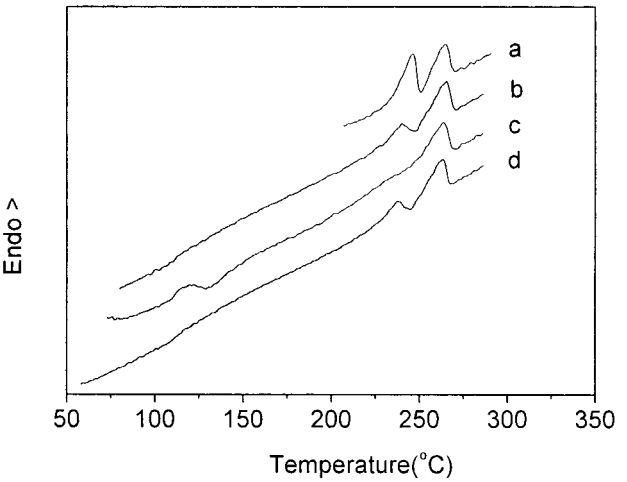

Figure 12 MDSC curves of 33% PHB polymer using different procedures (nonreversible heat flow).

that the transition from the one-dimensional nematic state to the two-dimensional smectic state is very easy.

To further confirm the above assumption, after Procedure b the sample was cooled quickly from 300°C to 50°C (referred to as Procedure c). Interestingly, the T_m1 transition disappeared, the T_m2 remained, and the glass-transition temperature was greatly strengthened. This indicates that crystallization could not occur under T_m1 upon quick cooling, whereas the smectic state could still form under T_m2. The decrease in the amount of crystals should result in an increase of the amorphous fraction.

To know whether the T_m1 transition was reversible, Procedure d was carried out following Procedure c. In fact, this procedure is the same as Procedure b except for the heating history. The same results were obtained, as expected (Fig. 10, curve d), suggesting that crystals will form under T_m1 on slowly cooling.

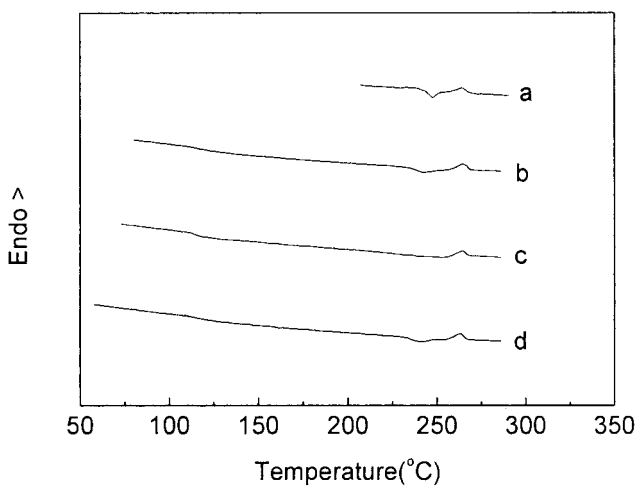

Figure 11 MDSC curves of 33% PHB polymer using different procedures (reversible heat flow).

The transition temperatures in the different heating procedures are summarized in Table V. It can be seen that the values of T_m2 changed very little (decreasing only 1°C), whereas those of T_m1 exhibited a greater change (ca. 8°C).

One of the important merits of the MDSC method is that it enables the total thermal effect to be divided into reversing and nonreversing thermal effects. In the thermograms of DSC (Figs. 7 and 9) and the total heat flow of MDSC (Fig. 10), it is not possible to clearly distinguish between the T_m1 and T_m2 transitions within the overall exothermal transition. However, in the reversing heat flow curve (Fig. 11), the recrystallization process between T_m1 and T_m2 can be clearly observed. In other words, the recrystallization process is at least partially reversible.

Moreover, Figures 11 and 12 show that the T_m2 transition obviously combined reversing and nonreversing thermal effects, but the T_m1 transition mainly had a nonreversing thermal effect, as the T_m1 transition in Figure 11 is not obvious. It could be suggested

TABLE V
Thermal Transition Temperatures of Polymers with Different Heating Procedures

Procedure	Heat flow	T_m1 (°C)	T_c (°C)	T_m2 (°C)
A	Total	245.3	—	264.9
	Reversible	—	247.7	—
	Nonreversible	246.2	—	264.2
B	Total	239.9	—	264.8
	Reversible	—	242.4	—
	Nonreversible	239.9	—	265.0
C	Total	None	—	263.8
	Reversible	—	None	—
	Nonreversible	None	—	263.7
D	Total	237.4	—	263.5
	Reversible	—	242.0	—
	Nonreversible	237.7	—	263.1

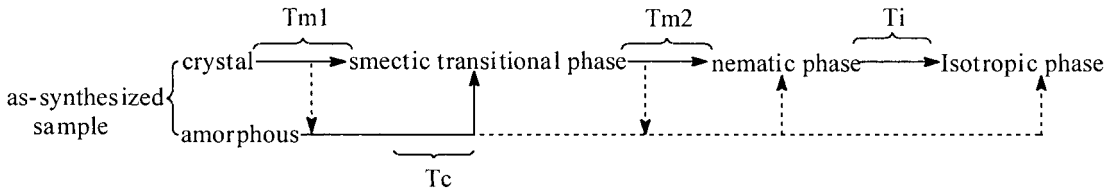

Scheme 4

that the irreversibility is the intrinsic reason for the testing-condition dependence of the T_m1 transition.

To our knowledge, many articles concerning the transition process of typical nematic thermotropic liquid crystal polymers have reported that on heating the DSC trace exhibited two melting endotherms corresponding to the transitions from solid state to liquid crystalline state and then to the isotropic liquid state. But this finding cannot be used to interpret the DSC and MDSC results in the current study.

According to the above results and analysis, an intermediate phase, the smectic transient state, probably should exist between the T_m1 and T_m2 transitions. According to this hypothesis, on heating, the transition process of this type of polymer would first be transformed from the (three-dimensional) solid state to the (two-dimensional) smectic transient state, then to the (one-dimensional) nematic liquid crystalline state, and finally to the isotropic liquid state. There is a recrystallization process between T_m1 and T_m2. The thermal transition model of this type of nematic liquid crystalline polymer is illustrated as Scheme 4, in which the dotted arrows indicate the possible phase transitions. In light of this model, it is likely that the spherulitelike feature observed by PLM was probably one texture of the crystalline state of this polymer.

CONCLUSIONS

A series of poly(ester imide ketone)s derived from *N*,*N*′-hexane-1,6-diylbis(trimellitimide), 4,4′-dihydroxybenzophenone, and *p*-hydroxybenzoic acid were synthesized by direct polycondensation method in BsCl, DMF, and Py with various contents of *p*-hydroxybenzoic acid. Significant nematic texture was observed using a hot-stage polarized light microscope. Most synthesized polymers show a nematic thermotropic liquid crystalline behavior. Under certain conditions, two completely different textures could be obtained for 33% PHB polymer. The polymers obtained were probably high-performance fiber materials because of the ease of forming tough fibers in the molten state. Thermogravimetric analysis study indicated that the polymers had good thermal stability. WAXD showed that the as-synthesized samples had some degree of crystallinity and that after a melting process, the phase structures changed greatly. The DSC and MDSC curves showed two endothermic peaks and an exothermic peak for the polymers with certain contents of PHB. The existence of a smectic transitional phase was confirmed by MDSC results. A phase transition model was proposed for this type of nematic liquid crystalline polymer to explain the complex thermal behavior. MDSC results also showed that the transition from solid state to smectic state was probably a nonreversible process.

Z.C. is grateful to Dr. Liu Tianxi from the Molecular & Bio-Materials Laboratory, National University of Singapore, for his kind help.

References

1. Kricheldorf, H. R. Advances in Polymer Science, Vol. 141; Springer-Verlag: Berlin, 1999.
2. Higashi, F.; Akiyama, N.; Takahashi, I.; Koyama, T. J. Polym Sci, Part A: Polym Chem 1984, 22, 1653.
3. Stanley, L. N. U.S. Pat. 3,073,866 (1963).
4. Kricheldorf, H. R.; Pakull, R. Macromolecules 1998, 21, 551.
5. Dong, D.; Zhuang, H.; Li, G.; Ni, Y.; Ding, M. J Polym Sci, Part A: Polym Chem 1999, 37, 211.
6. Chen, W.; Moon, I.-K.; Wunderlich, B. Polymer 2000, 41, 4119.